FULL PAPER

DOI: 10.1002/chem.200701208

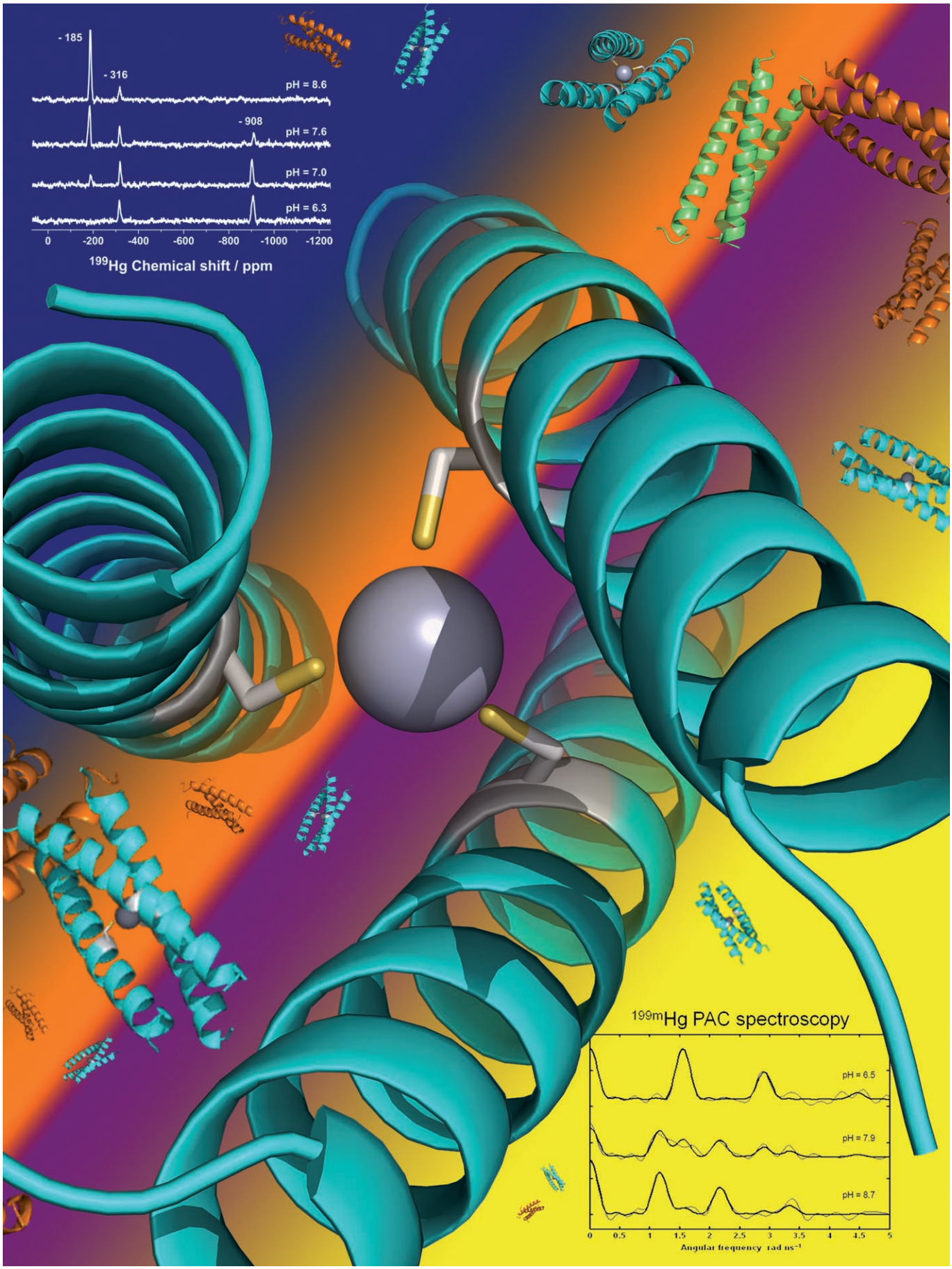

The Application of ^{199}Hg NMR and ^{199m}Hg Perturbed Angular Correlation (PAC) Spectroscopy to Define the Biological Chemistry of Hg^{II}: A Case Study with Designed Two- and Three-Stranded Coiled Coils

Olga Iranzo,[a] Peter W. Thulstrup,[b] Seung-baek Ryu,[c] Lars Hemmingsen,[b] and Vincent L. Pecoraro*[a, d]

Abstract: The use of de novo designed peptides is a powerful strategy to elucidate Hg^{II}–protein interactions and to gain insight into the chemistry of Hg^{II} in biological systems. Cysteine derivatives of the designed α-helical peptides of the TRI family [Ac-G-$(L_aK_bA_cL_dE_eE_fK_g)_4$-G-$NH_2$] bind Hg^{II} at high pH values and at peptide/Hg^{II} ratios of 3:1 with an unusual trigonal thiolate coordination mode. The resulting Hg^{II} complexes are good water-soluble models for Hg^{II} binding to the protein MerR. We have carried out a parallel study using ^{199}Hg NMR and ^{199m}Hg perturbed angular correlation (PAC) spectroscopy to characterize the distinct species that are generated under different pH conditions and peptide TRI L9C/Hg^{II} ratios. These studies prove for the first time the formation of [Hg{$(TRI\ L9C)_2$-(TRI L9C−H)}], a dithiolate–Hg^{II} complex in the hydrophobic interior of the three-stranded coiled coil $(TRI\ L9C)_3$. ^{199}Hg NMR and ^{199m}Hg PAC data demonstrate that this dithiolate–Hg^{II} complex is different from the dithiolate [$Hg(TRI\ L9C)_2$], and that the presence of third α-helix, containing a protonated cysteine, breaks the symmetry of the coordination environment present in the complex [$Hg(TRI\ L9C)_2$]. As the pH is raised, the deprotonation of this third cysteine generates the trigonal thiolate–Hg^{II} complex $Hg(TRI\ L9C)_3^-$ on a timescale that is slower than the NMR timescale (0.01–10 ms). The formation of the species [Hg{$(TRI\ L9C)_2$(TRI L9C−H)}] is the result of a compromise between the high affinity of Hg^{II} to form dithiolate complexes and the preference of the peptide to form a three-stranded coiled coil.

Keywords: coordination modes · mercury · metalloproteins · NMR spectroscopy · perturbed angular correlation (PAC) spectroscopy

[a] Dr. O. Iranzo, Prof. V. L. Pecoraro
Department of Chemistry, University of Michigan
Ann Arbor, Michigan 48109–1055 (USA)
Fax: (+1) 734-936-7628
E-mail: vlpec@umich.edu

[b] Prof. P. W. Thulstrup, Prof. L. Hemmingsen
Department of Natural Sciences
Faculty of Life Sciences, University of Copenhagen
Thorvaldsensvej 40, 1871 Frederiksberg (Denmark)

[c] S.-b. Ryu
Nuclear Solid-State Physics
Institute of Experimental Physics II
Faculty of Physics and Earth Sciences, Leipzig University
Linnestr. 5, 04103 Leipzig (Germany)

[d] Prof. V. L. Pecoraro
Biophysics Research Division, University of Michigan
Ann Arbor, Michigan 48109-1055 (USA)

Supporting information for this article is available on the WWW under http://www.chemeurj.org/ or from the author. It contains UV/Vis spectra of the complexes [$Hg(TRI\ L9C)_2$] and [Hg-$(TRI\ L9C)_2$(TRI L9C-H)] at pH 6.5.

Introduction

The biological chemistry of mercury is dominated by the coordination to sulfhydryl-containing ligands due to the high binding affinity of Hg^{II} for the soft and easily polarizable sulfur atom. Consequently, the high toxicity of this element, and its organic derivatives, is the result of its strong interaction with thiol-containing biomolecules such as proteins and glutathione.[1,2] Although Hg^{II}–thiolate bonds are thermodynamically very stable, their high lability and rapid ligand exchange causes the dispersion of Hg^{II} to random thiol ligands throughout the cell causing alterations in essential biochemical processes.[1–3] Not surprisingly, biological systems have responded to this toxicity with different strategies that share the same basic chemical principle: the strong affinity of Hg^{II} for thiol ligands. The strategy adopted by mammals mainly consists of Hg^{II} complexation and sequestration by metallothioneins, ubiquitous low-molecular-weight, cysteine-rich

proteins.[4] Bacteria achieve mercury resistance in a very different manner, having developed an elaborate system that transforms toxic Hg^{II}-containing compounds into Hg^0.[5–7]

Bacterial resistance to mercury is encoded by the Mer operon, with the expression of these detoxification proteins controlled by the metalloregulatory protein MerR. MerR is a homodimer bound to DNA in the presence or absence of Hg^{II}. In the absence of this metal, the MerR/DNA adduct adopts a conformation that represses gene transcription. Metal binding induces a conformational change of the Hg^{II}/MerR/DNA ternary complex leading to the unwinding of the DNA and subsequent transcription of the Mer genes. The MerR protein binds Hg^{II} with high specificity and affinity, responding to Hg^{II} at nanomolar concentrations. Each protein subunit of the MerR homodimer contains four cysteines, but site-directed mutagenesis studies revealed that only three of four cysteines are involved in binding.[8,9] These six cysteines (three per monomer) are located at the interface of the homodimer at which the actual binding site lies. The Hg^{II} ion is bound to only three of them, one cysteine from one monomer and two different cysteines from the other monomer, forming a mononuclear complex of trigonal geometry.[8–10] Given the inherent binding preferences with small molecules to form linear Hg–bis(thiolate) complexes ($\Delta G = -78$ kcal mol) versus the weaker affinity of the third thiolate to this linear moiety (≈ -1.2 kcal mol),[5] it is remarkable that MerR is able to sequester Hg^{II} in a trigonal structure at nanomolar concentrations. In addition to Hg^{II}, different levels of transcription in the presence of MerR have been observed in response to Cd^{II}, Zn^{II}, and Au^{I}.[11] However, higher concentrations of these other metal ions are required. This highlights the high degree of selectivity that metalloregulatory protein MerR possesses. In the case of Cd^{II}, a concentration two orders of magnitude higher than that for Hg^{II} was necessary for induction, reflecting the different affinity of these metals for thiolates and their geometric preferences. The Cd^{II} thiolate chemistry is dominated by tetrahedral $[Cd(SR)_4]^{2-}$ complexes and the thermodynamic barrier of dissociating a thiol from these complexes to form $[Cd(SR)_3]^-$ is higher than the barrier of adding an additional thiol to the linear species $[Hg(SR)_2]$.[5]

During the last decade, new insight into the Hg^{II}–thiol coordination environments in biological systems has been obtained by ^{199}Hg NMR spectroscopy. This spectroscopic technique has become a powerful structural tool for the characterization of metal-binding sites in metalloproteins. This utility is the result of the unique sensitivity of ^{199}Hg chemical shifts to the primary coordination sphere, including the nature of the donor ligand, the coordination number, and the geometry around the metal center; the ease of Hg^{II} substitution into the metalloprotein binding sites; and the fact that Hg^{II} can adopt the coordination environment of the native metal ion.[5,12–14] This spectroscopic technique has been a fundamental probe for understanding the structure and the molecular mechanism of action of the proteins involved in the bacterial mercury detoxification and biochemistry, such as MerR and MerP.[10,15,16] Additionally, ^{199}Hg NMR spectroscopy has been used to elucidate the coordination environment of copper, zinc, and iron metal ions in several metalloproteins.[10,17–21] There are now sufficient data in the literature regarding the ^{199}Hg chemical shifts of both small-molecule Hg^{II} complexes and proteins/peptides, that insight into the coordination environment of Hg^{II} can be obtained by simply correlating the observed ^{199}Hg chemical shift with those of structurally characterized compounds and proteins.

Another spectroscopic method that has been applied only to a limited number of metalloproteins, but promises to be an extremely powerful probe of Hg^{II} structure and dynamics in biological environments, is ^{199m}Hg perturbed angular correlation (PAC) spectroscopy.[22–24] In most biological applications of PAC spectroscopy the nuclear quadrupole interaction (NQI) is measured, providing a spectroscopic fingerprint of the local electronic and molecular structure and dynamics at the PAC probe site. ^{199m}Hg has been used as probe in studies of different systems, for example, the MerR and MerA proteins, rubredoxin and a number of small thiol-rich complexes. In all these cases, the combination of ^{199m}Hg PAC spectroscopy with other spectroscopic techniques has proven to be an effective way to study and determine the Hg^{II} coordination and geometry. In addition, the different timescale of these techniques can generate information that can be crucial for understanding the kinetics of conversion between the different species in solution. We expect that when used in conjunction, ^{199}Hg NMR and ^{199m}Hg PAC data will be as powerful a predictor of structure and dynamics as has been the combination of ^{113}Cd NMR and ^{111m}Cd PAC for thiolate-rich sites in protein molecules.[25–27]

An attractive strategy for elucidating Hg^{II}–protein interactions and to gain insight into the chemistry of Hg^{II} in biological environments is the use of de novo designed peptides. These peptides give rise to systems that are much simpler than the natural proteins they are mimicking, yet possess sufficiently more complexity than small inorganic model complexes. Therefore, de novo designed peptides that bind Hg^{II} through cysteine ligands can provide a good framework for studying structural and functional properties of the proteins involved in Hg^{II} complexation and its biological chemistry and toxicity. Our group has designed the amphipathic TRI peptide based on the heptad repeat strategy $(Ac\text{-}G\text{-}(L_aK_bA_cL_dE_eE_fK_g)_4\text{-}G\text{-}NH_2)$.[28,29] Substitution of a leucine for a cysteine in either position **a** or F generates peptides that in aqueous solution aggregate above pH 6.0, generating three-stranded coiled coils that contain a cysteine-rich binding site. The Hg^{II} complexes of these peptides $[Hg(TRI\ LXC)_3]^-$, in which LXC denotes that leucine in position X was replaced by cysteine, and related systems are good structural models for Hg^{II} bound to the metalloregulatory protein MerR.[25,28,30–32] UV/Vis, CD, EXAFS and ^{199}Hg NMR spectroscopic data are consistent with the binding of Hg^{II} in an uncommon trigonal environment. These results were particularly revealing, since few well-characterized, mononuclear, trigonal Hg^{II} thiolate complexes have been re-

ported to date, and these models are stable only in the solid state or nonaqueous environments.[33–36]

The pH dependence of the formation of such $[Hg(TRI\ LXC)_3]^-$ ($=[Hg(RS)_3]^-$) complexes reveals the release of a single proton with pK_a values around 7.6, for peptides in which cysteine is in position **a**, and around 8.5 for those in which cysteine is in position **d**.[25,30,32] Considering the pH dependence of the aggregation state of these TRI peptides in the presence and absence of Hg^{II}, two-stranded coiled coils at pH < 4 and three-stranded coiled coils at pH > 6 (Figure 1),[30] these results are consistent with the formation

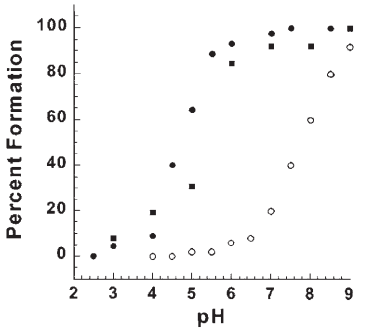

Figure 1. Percent formation versus pH plot for the formation of a three-stranded coiled coil in the absence of Hg^{II} from guanidinium denaturation studies (full circle); the formation of a three-stranded coiled coil in the presence of Hg^{II} from size-exclusion chromatography (full square); and the formation of trigonal thiolate–Hg^{II} within the interior of a three-stranded coiled coil (empty circle).[30]

of a dithiolate–Hg^{II} ion encapsulated within a three-stranded coiled coil $[Hg\{(TRI\ LXC)_2(TRI\ LXC{-}H)]$ ($=[Hg(RS)_2(RSH)]$), and deprotonation of the third thiol group to form the trigonal thiolate–Hg^{II} $[Hg(TRI\ LXC)_3]^-$, as pH is raised (see Scheme 1). A significant question regarding this system that still remains unanswered is the geometric nature of the dithiolate–Hg^{II} within the three-stranded coiled coils. In the course of our attempts to understand and characterize the different Hg^{II} species that are generated under different ex-

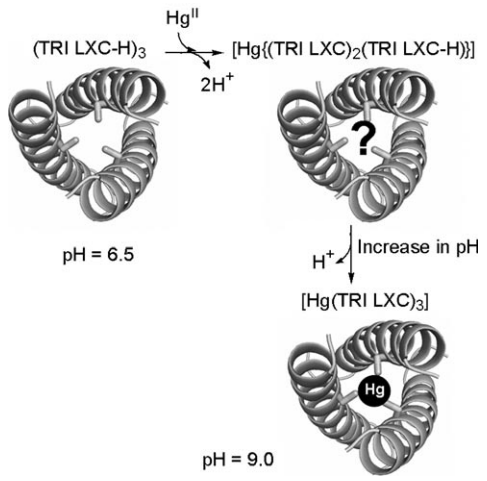

Scheme 1. The pH-dependent binding of Hg^{II} to the TRI peptide family.

perimental conditions of pH and peptide/Hg^{II} ratios fully, we have carried out a parallel study using ^{199}Hg NMR and ^{199m}Hg PAC spectroscopy to analyze the binding of Hg^{II} to the peptide TRI L9C. The results presented here support the existence of a dithiolate–Hg^{II} complex encapsulated within a three-stranded coiled coil and the stepwise aggregation–deprotonation mechanism we proposed previously.[30] These data underscore the important synergistic role that ^{199m}Hg PAC and ^{199}Hg NMR spectroscopy can play in determining the solution structure of mercury binding sites in biopolymers and de novo designed proteins/peptides.

Results

^{199}Hg NMR spectroscopy: A coaxial NMR tube containing $^{199}Hg(NO_3)_2$ (12.1 mM) and three equivalents of the **d** site peptide TRI L19C at pH 9.6 was used as an external reference ($\delta = -316$ ppm) for all the ^{199}Hg NMR experiments. Figure 2 shows the ^{199}Hg NMR spectra corresponding to sol-

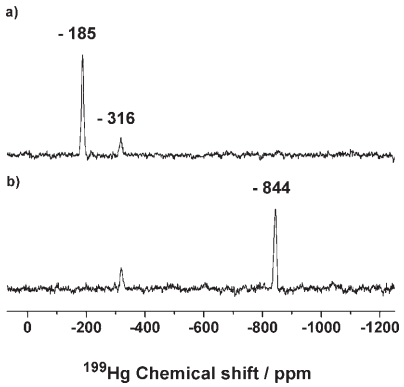

Figure 2. ^{199}Hg NMR spectra at pH 8.6 of solutions containing: a) 4.9 mM $^{199}Hg(NO_3)_2$ and three equivalents of TRI L9C; b) 7.9 mM $^{199}Hg(NO_3)_2$ and two equivalents of TRI L9C. The signal at −316 ppm corresponds to the external standard ($[Hg(TRI\ L19C)_3]^-$ pH 9.6).

utions containing different ratios of the peptide TRI L9C and $^{199}Hg^{II}$ at pH 8.6. These experiments were carried out at this basic pH value, since our previous pH-dependence studies of Hg^{II} complexation by TRI peptides containing the cysteine moiety in position **a** showed the complete formation of the trigonal thiolate–Hg^{II} ($[Hg(TRI\ LXC)_3]^-$) by pH 8.5.[25,30,32] A single resonance is observed for the sample with a 3:1 TRI L9C/Hg stoichiometry (Figure 2a) with a chemical shift of $\delta = -185$ ppm. Based on the previous results obtained for the TRI and Coil-Ser family of peptides,[28,32] these data are consistent with a three-sulfur environment and indicate the formation of the complex $[Hg(TRI\ L9C)_3]^-$. A single resonance is also observed for the sample with a 2:1 TRI L9C/Hg stoichiometry (Figure 2b), but in this case with a chemical shift of $\delta = -844$ ppm, which is very close to the value observed previously for the peptide TRIL16C under the same experimental conditions ($\delta = -834$ ppm).[28] These resonances are shifted upfield from the

signal observed for the trigonal thiolate–Hg^{II} complexes, but within the chemical shift range of $\delta = -760$ to -1200 ppm expected for dithiolate–Hg^{II} complexes.[5,13] This observation leads to the simple assumption that Hg^{II} is bound to two thiol groups indicating the formation of the complex [Hg(TRI L9C)$_2$].

Shown in Figure 3 are the ^{199}Hg NMR spectra corresponding to the pH titration of a solution containing 4.9 mM ^{199}Hg(NO$_3$)$_2$ and three equivalents of TRI L9C. A single resonance is observed at low pH with a chemical shift of $\delta = -908$ ppm, which is within the range expected for dithiolate–Hg^{II} complexes and suggests the presence of this type of complex as the sole species in solution. As the pH value of the solution is increased, the intensity of this resonance decreases and a new resonance appears with a chemical shift of $\delta = -185$ ppm. At pH 8.6, only the resonance at $\delta = -185$ ppm, which corresponds to the formation of the complex $[Hg(TRI\ L9C)_3]^-$, is observed. The fact that for a specific pH value both resonances, $\delta = -185$ and -908 ppm, are simultaneously observable in solution indicates that these two Hg^{II} complexes interconvert slowly on the NMR timescale at the pH values studied. Using the area of the external standard as a reference value, the integration obtained for the two species in solution at the different pH values show that the conversion of the dithiolate to the trigonal thiolate–Hg^{II} complex occurs with an apparent pK_a value of 7.6. Note here that the ^{199}Hg chemical shift obtained at low pH is slightly shifted upfield from the one observed in Figure 2b suggesting the formation of a different Hg^{II}–bis(thiolato) complex; however, since these experiments were carried out at different pH conditions, these observations could result from the difference in acidity of the samples. In order to assess whether the change observed in the ^{199}Hg chemical shift ($\delta = -908$ vs -844 ppm) is due to a change in pH or to a different environment around Hg^{II}, a sample containing two equivalents of TRI L9C and one equivalent of Hg^{II} was prepared at pH 6.3 and analyzed by ^{199}Hg NMR spectroscopy. A single resonance is observed with a chemical shift of $\delta = -844$ ppm, which is the same value observed in the spectrum shown in Figure 2b. This experiment demonstrates that the differences in chemical shift are structural and not due to pH changes alone.

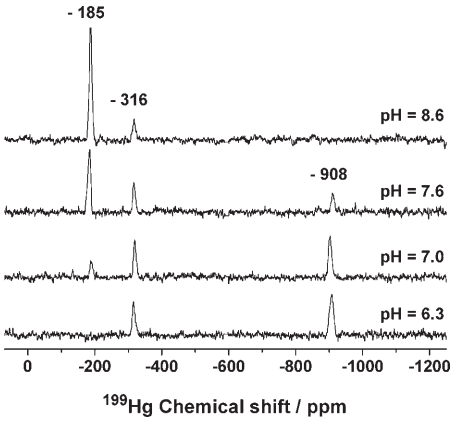

Figure 3. ^{199}Hg NMR spectra of solutions containing 4.9 mM ^{199}Hg(NO$_3$)$_2$ and three equivalents of TRI L9C at different pH values. The signal at -316 ppm corresponds to the external standard ($[Hg(TRI\ L19C)_3]^-$ pH 9.6).

UV/Vis spectroscopy: The UV/Vis spectra of solutions at pH 6.5 containing one equivalent of Hg^{II} (20 μM) and either two equivalents of TRI L9C, conditions favoring the formation of the complex [Hg(TRI L9C)$_2$], or three equivalents of TRI L9C, conditions favoring the formation of the complex [Hg{(TRI L9C)$_2$(TRI L9C–H)}], show the signature charge-transfer band at 240 nm characteristic of the formation of dithiolate–Hg^{II} complexes (HgS_2) (Figure S1 in the Supporting Information).[28]

^{199m}Hg perturbed angular correlation (PAC) spectroscopy: ^{199m}Hg PAC spectroscopy was used to determine the Hg^{II} coordination geometry of the different Hg^{II} complexes of TRI L9C observed by ^{199}Hg NMR spectroscopy. Figure 4 shows the Fourier transforms of the ^{199m}Hg PAC spectra corresponding to the pH titration of a solution containing the peptide TRI L9C and Hg^{II} at a peptide/Hg^{II} ratio of 12:1. The data were analyzed as described in the Experimental Section. All three spectra were fitted with two nuclear quadrupole interactions (NQIs) and each NQI was modeled by using a separate set of parameters that includes ν_Q, η, δ, $1/\tau_c$, and A. The parameters fitted to these PAC data are reported in Table 1 (rows 1–3). Only one NQI with a significant amplitude (A) was found for the experiment at pH 6.5. This set of signals (NQI1) corresponds to a ν_Q of 1.558 GHz and an η of 0.23. These fitted PAC parameters compare reasonably well with the literature data for a model compound with a two-coordinate, almost linear S-Hg-S structure, see Table 2, although ν_Q is higher.[37] When the pH is increased, another set of signals appears in the PAC spectra (NQI2) and at pH 8.7 this constitutes the major part of the signal.

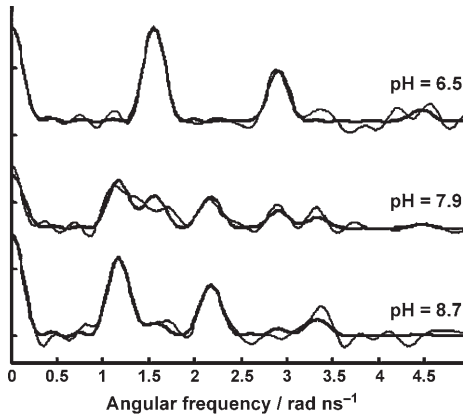

Figure 4. ^{199m}Hg PAC spectra of solutions containing TRI L9C (125–130 μM) and $HgCl_2$ (10.8 μM) at different pH values. The thin lines represent the Fourier transform of the experimental data and the bold lines represent the fit.

Table 1. Parameters fitted to the PAC data.[a]

Peptide (c [μM])	Ratio TRI L9C/Hg^{II}	pH	ν_Q [GHz]	η	$\delta\times100$	$1/\tau_c$ [μs^{-1}]	$A\times100$	χ^2_r
TRI L9C (130)	12	6.5	1.558(7)[b]	0.23(1)	0(1)	19(13)	10.7(0.6)	0.78
TRI L9C (130)	12	7.9	1.164[c,g]	0.25[g]	0.0[g]	22[g]	5.3(2)	0.80
			1.558[c,g]	0.23[g]	0.0[g]	22[g]	3.7(3)	
TRI L9C (125)	12	8.7	1.164(5)[d]	0.25(2)	0(1)	22(11)	8.6(4)	0.86
			1.558[d,g]	0.23[g]	0.0[g]	22(11)	1.3(4)	
TRI L9C (128)	2	8.1	1.529(9)[e]	0.13(3)	2.1(9)	25(12)	12.2(6)	0.78
TRI L9C (126)	2	6.6	1.539(10)[f]	0.11(3)	2.9(9)	10(10)	10.6(5)	0.72

[a] The numbers in parenthesis are the standard deviations of the fitted parameters. [b] $\omega_1=1.551(9)$ rad ns^{-1}. [c] $\omega_1=1.167$[f] rad ns^{-1} and $\omega_1=1.551$[f] rad ns^{-1}. [d] $\omega_1=1.167(8)$ rad ns^{-1} and $\omega_1=1.551$[f] rad ns^{-1}. [e] $\omega_1=1.467(9)$ rad ns^{-1}. [f] $\omega_1=1.471(9)$ rad ns^{-1}. [g] Fixed in the fit.

Table 2. NQI parameters of the different Hg^{II}–thiolate complexes of known structures.

Complexes	ν_Q [GHz]	η	Coordination geometry	Ref.
$[Hg(cysteine)_2]$	1.41(2)[b]	0.15(2)	distorted linear, 2 thiolates	[37]
MerA (77 K)	1.42(6)[a,c]	0.15(1)	distorted linear, 2 thiolates	[39]
$[NBu_4][Hg(SPh)_3]$	1.16(1)[d]	0.31(1)	distorted trigonal, 3 thiolates	[24]
MerR (77 K)	1.18(1)[a,e]	0.25(1)	distorted trigonal, 3 thiolates	[39]
MerR (0 °C, sat. sucrose)	1.16(1)[a,f]	0.22(1)	distorted trigonal, 3 thiolates	[39]
$[Hg(S\text{-}t\text{Bu})_2]$	0.35(1)[g]	0 (fixed)	distorted tetrahedral, 4 thiolates	[37]
Hg–rubredoxin	0.10(2)[a,h]	0 (fixed)	distorted tetrahedral, 4 thiolates	[63]

[a] The standard deviations were determined assuming that $s_{\omega1}/\omega_1=s_{\nu Q}/\nu_Q$, with values of $s_{\omega1}$ and ω_1 from the cited references. [b] $\omega_1=1.36(2)$ rad ns^{-1}. [c] $\omega_1=1.375(26)$ rad ns^{-1}. [d] $\omega_1=1.20(1)$ rad ns^{-1}. [e] $\omega_1=1.19(1)$ rad ns^{-1}. [f] $\omega_1=1.15(1)$ rad ns^{-1}. [g] $\omega_1=0.33(1)$ rad ns^{-1}. [h] $\omega_1=0.09(2)$ rad ns^{-1}.

To determine the NQI2 parameters, the data recorded at pH 8.7 were fitted keeping the parameters for NQI1 fixed, except for the amplitude A and $1/\tau_c$, which is constrained to be the same for the two NQIs. In this case, the fitted PAC parameters ($\nu_Q=1.164$ GHz and $\eta=0.25$) compare excellently with literature data for a trigonal-planar $[Hg(RS)_3]^-$ coordination geometry,[24] see Table 2. Finally, the data recorded at pH 7.9 were fitted with NQI1 and NQI2 fixed, except for the amplitudes. The amplitudes of the two NQIs at the three pH values indicate that a group with a pK_a of about 7.8 is being titrated.

The PAC data that correspond to a solution containing the peptide TRI L9C and Hg^{II} at a peptide/Hg^{II} ratio of 2:1 at pH value of 8.1 are shown in Figure 5a. The fitted parameters obtained for this NQI ($\nu_Q=1.529$ GHz and $\eta=0.13$) appear to reflect a linear $[Hg(RS)_2]$ coordination geometry. Surprisingly, this signal is slightly different from that found at low pH and a TRI L9C/Hg^{II} ratio of 12:1 (Figure 5b), which is also interpreted as a linear $[Hg(RS)_2]$ coordination geometry as described above. To test if the change in these NQIs is due to the different pH values used in the experiments (8.1 versus 6.5), a sample with a TRI L9C/Hg^{II} ratio of 2:1 and pH value of 6.6 was prepared and analyzed by PAC spectroscopy (Figure 5c). Although the NQI parameters changed slightly upon the decrease in pH ($\nu_Q=1.539$ GHz and $\eta=0.11$), they are very similar to those found at pH 8.1 with a TRI L9C/Hg^{II} ratio of 2:1, and still significantly different, with lower values for ν_Q and η, from those found at pH 6.5 with a TRI L9C:Hg^{II} ratio of 12:1 ($\nu_Q=1.558$ GHz and $\eta=0.23$). These results indicate that the differences observed in the fitted parameters are mainly the consequence of a different geometric environment around the Hg^{II} ion and not due to the change in pH. This conclusion is fully consistent with the ^{199}Hg NMR data described above.

Discussion

We have been interested in defining the chemistry of Hg^{II} with proteins in order to establish how this metal may be responsible for toxicity in bacteria and mammals. In addition, these studies aim to provide a basis for a better understanding of the sequestration of Hg^{II} and of the detoxification systems that biological systems have develop to overcome the detrimental effects of this metal. In previous studies, we have shown that the cysteine derivatives of the de novo designed TRI and related peptides can be used to generate stable water-soluble peptidic models for Hg^{II} binding to the protein MerR.[25,28,30–32] The binding affinity of Hg^{II} to the TRI family of peptides is high with micromolar dissociation constants,[31] and one of these peptides, Grand L9C, is capa-

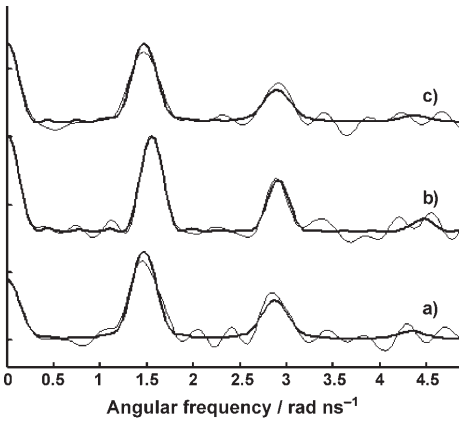

Figure 5. ^{199m}Hg PAC spectra of solutions containing TRI L9C (125–130 μM) at different pH values and different ratios of $HgCl_2$: a) TRI L9C/Hg^{II} ratio of 2:1 at pH 8.1; b) TRI L9C/Hg^{II} ratio of 12:1 at pH 6.5; and c) TRI L9C/Hg^{II} ratio of 2:1 at pH 6.6. The thin lines represent the Fourier transform of the experimental data and the bold lines represent the fit.

ble of displaying ≈50% trigonal Hg^{II} formation at nanomolar metal concentrations.[31] This affinity is remarkably similar to the MerR protein, which also possesses nanomolar Hg^{II} ion sensitivity.[8,36] This natural metalloprotein, as well as our designed peptides, use the strategy of increasing the effective molar volume of thiolate ligands around Hg^{II} to achieve the unusual trigonal coordination geometry at nanomolar concentrations and stoichiometric protein/metal ratios.

However, the pH dependence studies of the binding of Hg^{II} to the TRI peptides in conjunction with the pH dependence studies of the aggregation state of these TRI peptides, in the absence and presence of Hg^{II}, have shown that the spatial arrangement of three thiols is not the only factor determining the formation of the trigonal thiolate–Hg^{II}. Figure 1 shows that the transition between two and three-stranded coiled coils in the presence of Hg^{II} follows the pH profile observed in the absence of the metal, and this occurs well below the pH range observed for the transition of linear to trigonal thiolate–Hg^{II}. Up to now, our best description for this behavior is shown in Scheme 1, in which we propose the presence of a dithiolate–Hg^{II} complex in the interior of the three-stranded coiled coil, followed by the deprotonation of the third cysteine thiol group to form the trigonal Hg^{II} complex $[Hg(TRI\ LXC)_3]^-$ when pH is increased.[30] Nonetheless, our current data do not allow us to propose a geometric structure for the complex [Hg{(TRI LXC)$_2$(TRI LXC−H)}]. Therefore, an important issue that still needs to be addressed to validate this mechanism is the geometric nature of dithiolate–Hg^{II} complex [Hg{(TRI LXC)$_2$(TRI LXC−H)}]. Is the [Hg{(TRI LXC)$_2$-(TRI LXC−H)}] complex completely different from the linear dithiolate $[Hg(TRI\ LXC)_2]$? What is the effect, if any, of having a thiol group in close proximity to a Hg^{II} bound to two thiolates?

To gain insight into these species, we have analyzed the binding of Hg^{II} to TRI L9C under different peptide/Hg^{II} ratios and pH conditions. We turned to ^{199}Hg NMR spectroscopy, since this technique has been successfully applied to elucidate the primary coordination sphere and geometry of Hg^{II} in different biological environments.[15,17–21] We have already shown that this technique can be applied in our systems, the TRI family of peptides and derivatives, to distinguish between two and three thiolates bound to the Hg^{II} ion.[28,32,38] In particular, the ^{199}Hg chemical-shift range observed for the complexes $[Hg(TRI\ LXC)_3]^-$ and [Hg-(TRI LXC)$_2$] is from −179 to −320 and from $\delta = -830$ to −950 ppm, respectively. Consistent with these data, the ^{199}Hg chemical shifts shown in Figure 2 are indicative of the formation of the dithiolate–Hg^{II} complex $[Hg(TRI\ L9C)_2]$ ($\delta = -844$ ppm), when the ratio TRI L9C/Hg is 2:1, and of the trigonal thiolate–Hg^{II} complex $[Hg(TRI\ L9C)_3]^-$ ($\delta = -185$ ppm), when the ratio TRI L9C/Hg is 3:1. These results corroborate our previous UV/Vis spectroscopic analyses,[31] and, once more, they highlight how Hg^{II} ions are able to control the aggregation state of the peptide TRI L9C. On the basis of the different ^{199}Hg chemical shifts expected for two or three thiolates bound to Hg^{II}, we postulated that a ^{199}Hg NMR pH titration under conditions in which the peptide TRI L9C forms a three-stranded coiled coil (ratio TRI L9C/Hg = 3:1) could give us crucial information regarding the different Hg^{II} species that exist in solution as pH is raised from 6.3 to 8.6. This knowledge will allow us to understand the behavior shown in Figure 1. The single resonance observed at pH 6.3 with a ^{199}Hg chemical shift of $\delta = -908$ ppm indicates the formation of a dithiolate–Hg^{II} complex as the only species in solution (Figure 3). The fact that no other resonance is observed down to $\delta = 80$ ppm, besides the external standard at $\delta = -316$ ppm, suggest that no trigonal thiolate–Hg^{II} complex is formed under these conditions. This result supports what it is predicted, at that pH value, by the data shown in Figure 1 and the hypothesis that, under these conditions, there is a three-stranded coiled coil containing Hg^{II} bound to two cysteines ([Hg-{(TRI L9C)$_2$(TRI L9C-H)}]). Consistent with the same data, the increase in pH causes the conversion of the dithiolate–Hg^{II} complex ($\delta = -908$ ppm) into the trigonal thiolate–Hg^{II} complex $[Hg(TRI\ L9C)_3]^-$ ($\delta = -185$ ppm), which is the final species in solution at high pH. These results explain why all the pH profiles observed for the formation of the trigonal thiolate–Hg^{II} in the TRI peptide family and derivatives are consistent with the release of a single proton.[25,30–32] This proton belongs to the deprotonation of the third thiol in the complex [Hg{(TRI L9C)$_2$-(TRI L9C−H)}] to form the respective trigonal thiolate complex $[Hg(TRI\ L9C)_3]^-$. The pK_a value of 7.6 determined by the ^{199}Hg NMR pH titration is in agreement with the value obtained from UV/Vis pH titration experiments (p$K_a = 7.6 \pm 0.2$).[30]

The presented data support the hypothesis of the formation of a dithiolate–Hg^{II} within a three-stranded coiled coil. Based on the ^{199}Hg NMR data shown in Figure 6, this dithiolate–Hg^{II} is different from the species observed at the same pH when the ratio TRI L9C/Hg is 2:1. We next analyzed these Hg^{II} complexes by UV/Vis spectroscopy to determine if these structures could be resolved. However, these UV/

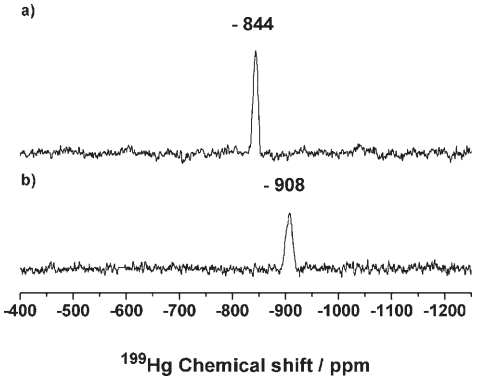

Figure 6. ^{199}Hg NMR spectra at pH 6.3 of solutions containing: a) 7.9 mM $^{199}Hg(NO_3)_2$ and two equivalents of TRI L9C; b) 4.9 mM $^{199}Hg(NO_3)_2$ and three equivalents of TRI L9C.

Vis spectra are too similar to infer any conclusion regarding possible differences in the structure of the complexes (Figure S1 in Supporting Information). Clearly, using only the NMR and UV/Vis data it is very hard to establish the identity of the species yielding the different ^{199}Hg chemical shifts and to interpret the geometry around the Hg^{II}.

^{199m}Hg PAC spectroscopy is a powerful tool for distinguishing between two, three, and four sulfur atoms bound to Hg^{II} and for obtaining information regarding structural distortions for a given coordination number.[39] It has been successfully applied to study the coordination number and geometry of the Hg^{II} ion in different Hg^{II} complexes, including small inorganic complexes and proteins (Table 2).[22,39,40] The metalloregulatory protein MerR is one of the systems studied by this technique and the PAC parameters obtained indicate unambiguously that Hg^{II} is bound to three thiolates, supporting the previous UV/Vis, EXAFS, and ^{199}Hg NMR data.[10,36,41] Since the Hg^{II} complexes of the TRI peptide family ($[Hg(TRI\ LXC)_3]^-$) are good structural models for Hg^{II} bound to MerR, we anticipated that this technique could provide us crucial insights regarding the structure of our different Hg^{II} species. The PAC parameters ($\nu_Q =$ 1.164 GHz and $\eta = 0.25$) obtained for a sample containing the peptide TRI L9C and Hg^{II} under conditions in which the complex $[Hg(TRI\ L9C)_3]^-$ is formed (peptide/Hg^{II} ratio of 12:1 and high pH) compare very well with published data for Hg^{II} complexes with a trigonal-planar $[Hg(RS)_3]^-$ coordination geometry (Table 2). Our results agree with those reported for MerR ($\nu_Q = 1.16$ GHz and $\eta = 0.22$) showing that our system is a good structural model for Hg^{II} bound to this protein. This observation corroborates our previous studies in which we demonstrated that the TRI peptide family bind Hg^{II} in a very similar way as MerR is proposed to do.[25,28,30–32] The PAC parameters ($\nu_Q = 1.529$ GHz and $\eta =$ 0.13) obtained under similar conditions but with a peptide/Hg^{II} ratio of 2:1 are in agreement with published values for Hg^{II} complexes with a linear $[Hg(RS)_2]$ coordination geometry (Table 2). These PAC parameters showed nearly no variation with pH (see Table 1 rows 4 and 5) indicating that a linear $[Hg(TRI\ L9C)_2]$ complex is always observed in the pH range studied. This result is consistent with our previous studies in which the formation of the trigonal thiolate–Hg^{II} was never observed at peptide/Hg ratio of 2 regardless of pH, concentration or peptide sequence,[25,28,30–32] reflecting the higher tendency of Hg^{II} to form Hg–bis(thiolate) complexes ($\Delta G = -78$ kcal mol^{-1}).[5] These results show how ^{199m}Hg PAC spectroscopy is able to distinguish clearly between linear and trigonal Hg^{II} complexes in our TRI peptide system.

We next examined a ^{199m}Hg PAC pH titration under conditions in which the peptide TRI L9C forms a three-stranded coiled coil to identify the Hg^{II} species observed in the ^{199}Hg NMR pH titration shown in Figure 3. In particular, we were interested in differentiating between the coordination environment of the two different dithiolate–Hg^{II} complexes, $[Hg(TRI\ L9C)_2]$ and $[Hg(TRI\ L9C)_2(TRI\ L9C{-}H)]$. In agreement with the ^{199}Hg NMR results, only two different species are observed in a solution containing a TRI L9C/Hg ratio of 12:1 in the pH range from 6.5 to 8.7 (Figure 4). At low pH there is only one set of signals that correspond to a NQI with a ν_Q of 1.558 GHz and an η of 0.23. When the pH is increased, another set of signals appears in the PAC spectra with a ν_Q of 1.164 GHz and an η of 0.25. This species is the major one (90%) present in solution at pH 8.7 and the fitted PAC parameters indicate the formation of a complex with a trigonal-planar $[Hg(RS)_3]^-$ coordination geometry (Table 2), which is in agreement with the ^{199}Hg NMR data obtained for the complex $[Hg(TRI\ L9C)_3]^-$ at high pH ($\delta = -185$ ppm). The fitted PAC parameters for the species at low pH compare reasonably well with published data for linear $[Hg(RS)_2]$ coordination geometry supporting the formation of a dithiolate–Hg^{II}. These data are consistent with the ^{199}Hg chemical shift of $\delta = -908$ ppm observed at low pH. Nonetheless, our dithiolate–Hg^{II} complex encapsulated in the three-stranded coiled coil, $[Hg\{(TRI\ L9C)_2(TRI\ L9C{-}H)\}]$, shows a higher value of η than those previously reported for linear $[Hg(RS)_2]$ coordination geometries (see Table 2). This parameter, η, is the asymmetry factor and it is a measure of the deviation from axial symmetry. The η parameter is always between 0 and 1, with a value of 0 in pure axially symmetry. Therefore, the higher value of η observed for $[Hg\{(TRI\ L9C)_2(TRI\ L9C{-}H)\}]$ is indicative of a lower degree of symmetry around the axis S-Hg-S. This can be explained in three different ways:

1) The species $[Hg[(TRI\ L9C)_2(TRI\ L9C\text{-}H)]]$ can contain a Hg^{II} ion bound to two thiolates ($Hg(RS)_2$) and a weak bond between the metal and the sulfur atom of the thiol group of the third cysteine ($RSH\cdots Hg(RS)_2$). This interaction will break the axial symmetry around the axis S-Hg-S in the complex $[Hg(RS)_2]$.
2) There is a fast equilibrium that involves Hg^{II} and the proton moving rapidly from sulfur-to-sulfur among the three possible choices. In this case, the protonated sulfur will not be coordinated to the Hg^{II}, but due to the dynamics of the process, the Hg^{II} bound to two thiolates will never become linear. This equilibrium could explain why the ^{199}Hg NMR resonance corresponding to the complex $[Hg\{(TRI\ L9C)_2(TRI\ L9C{-}H)]$ ($\nu_{1/2} = 1329$ Hz) is broader than the one corresponding to $[Hg(TRI\ L9C)_2]$ ($\nu_{1/2} = 950$ Hz). However, the PAC timescale may be short enough ($\approx$ns) to record a snapshot of one of the three possible configurations.
3) The protonated sulfur does not bind to the Hg^{II} at all and the distortion is because a three-stranded coiled coil does not allow the cysteine sulfur atoms to adopt conformers that yield as linear a structure as does the more flexible two-stranded coiled coil.

Based on the small changes observed in both the ^{199m}Hg PAC (Figure 5) and ^{199}Hg NMR (Figure 6) spectra of the two dithiolate–Hg^{II} complexes, $[Hg\{(TRI\ L9C)_2(TRI\ L9C{-}H)\}]$ and $[Hg(TRI\ L9C)_2]$, it seems likely that the third thiol is not coordinating to the Hg^{II} ion. Hence, the less likely

possibility is the first one; however, the data we have do not allow us to completely rule the first option out.

A different environment around the Hg^{II} ion should be expected for the complex $[Hg(TRI\ L9C)_2]$, in which the third thiol is absent, in comparison with the one observed for the species $[Hg\{(TRI\ L9C)_2(TRI\ L9C{-}H)\}]$. The ^{199m}Hg PAC data obtained for the experiment carried out at pH 6.6 with a TRI L9C/Hg ratio of 2:1 shows a lower value of η (= 0.11). This η value supports a higher degree of symmetry around the S-Hg-S axis, which is consistent with the absence of the third thiol and, therefore, a two-stranded coiled-coil structure that can accommodate the linear structure better than a three-stranded coiled coil. This value is in complete agreement with those reported in Table 2 for almost linear dithiolate–Hg^{II} complexes. The values obtained for the parameter ν_Q in both dithiolate–Hg^{II} complexes, $[Hg(TRI\ L9C)_2]$ ($\nu_Q = 1.558$ GHz) and $[Hg\{(TRI\ L9C)_2(TRI\ L9C\text{-}H)\}]$ ($\nu_Q = 1.529/1.539$ GHz) are slightly higher than those reported for other dithiolate–Hg^{II} complexes (see Table 2). One possible explanation is a shorter Hg–S bond length in our TRI systems, since the value of ν_Q is expected to depend on this distance roughly as r^-3, as has been demonstrated for Cd^{II} complexes.[42] Previous EXAFS data have shown a Hg–S bond length of 2.30 Å for the similar complex $[Hg(TRI\ L16C)_2]$,[28] which is slightly shorter than the distances reported for the $[Hg(Cys)_2]$ complex (2.355 and 2.329 Å)[43] shown in Table 2. Using a scaling factor of $(2.30/2.35)^3$, the ν_Q of 1.558 GHz is reduced to 1.46 GHz, and the ν_Q of 1.529 GHz is reduced to 1.43 GHz, both in excellent agreement with the data from the small reference compounds. This shorter bond could be the result of the coiled-coil structure itself that keeps the cysteine moieties closer.

Based on the ^{199m}Hg PAC data, the conversion between these two species, $[Hg\{(TRI\ L9C)_2(TRI\ L9C\text{-}H)\}]$ and $[Hg(TRI\ L9C)_3]^-$, occurs with a pK_a of 7.8, a value that agrees within ± 0.2 with the pK_a values determined independently by ^{199}Hg NMR in this work ($pK_a = 7.6 \pm 0.2$) and by UV/Vis pH titrations in previous studies ($pK_a = 7.6 \pm 0.2$).[30] An interesting observation is the fact that the conversion between these two species is slow both on the ^{199}Hg NMR and ^{199m}Hg PAC timescales. Both techniques show the presence of two unique species in solution that interconvert as pH is raised, since the disappearance of the spectroscopic features corresponding to $[Hg\{(TRI\ L9C)_2(TRI\ L9C\text{-}H)\}]$ parallels the appearance of those corresponding to $[Hg(TRI\ L9C)_3]^-$. Considering the NMR (0.01–10 ms) and PAC (0.1–100 ns) timescales, these results indicate that the conversion between these species is slower than ms. These data contrast with the known lability of mercury thiolates under conditions of excess thiol, in which ligand exchange has been proposed to occur by the formation of the reactive $[Hg(RS)_3]^-$ intermediate.[44] For example, for the ligand glutathione (GSH) the average lifetime of the species $[Hg(SG)_3]^-$ (SG = glutathionate) at pH 7 was 1.4×10^{-4} s. The rates of loss of the third thiolate GS^- or thiol GSH ligand to generate the complex $[Hg(GS)_2]$ were determined to be $6.3 \times 10^3\ s^{-1}$ and $6.3 \times 10^9\ M^{-1}\ s^{-1}$, respectively. In our case, the dissociation of the third thiol/thiolate from Hg^{II} in the species $[Hg(TRI\ L9C)_3]^-$ to generate $[Hg\{(TRI\ L9C)_2(TRI\ L9C{-}H)\}]$ occurs on the ms timescale or longer. This slower exchange is mainly due to the inherent structure of these peptides that makes the trigonal Hg^{II} complexes much more stable and less prone to ligand exchange than in the case of glutathione, since the dissociated thiol/thiolate ligand remains in close proximity to the $\{Hg(RS)_2\}$ moiety, facilitating thus the reformation of the trigonal thiolate mercury complex. Consistent with these observations, in solutions containing mixtures of different Hg^{II} complexes of TRI and derivative peptides, the different Hg^{II} species do not exchange or, if they do, the ligand exchange occurs at a much slower rate than ms.[32,45] In all cases, the ^{199}Hg NMR resonances corresponding to the different species in solution were always observable at room temperature, and no average isotropic shifts or coalesced resonances were obtained.

We have previously examined the reaction of Cd^{II} with related peptides using ^{113}Cd NMR and ^{111m}Cd PAC spectroscopy.[25,27] For the peptide TRI L16C, a single ^{113}Cd NMR resonance was observed at $\delta = 625$ ppm for $[Cd(TRI\ L16C)_3]^-$ at pH 8.5; however, ^{111m}Cd PAC spectroscopy demonstrated that there were two species in solution. The major species corresponded to a pseudo-tetrahedral CdS_3O^- complex and the minor component was a trigonal CdS_3^- site. Under these conditions, the two species were under fast exchange on the NMR timescale, but slow exchange on the PAC timescale. The best model for this system was a rapid water exchange that interconverted the three- and four-coordinate sites quickly. In contrast, if mixtures of the related peptide systems $[Cd(CS\,L9C)_3]^-$ and $[Cd(CS\,L19C)_3]^-$ were simultaneously present in solution, then two ^{113}Cd resonances at $\delta =$ 602 and 628 ppm were observed, each corresponding to a fast-exchanging CdS_3/CdS_3O site.[32] Similarly, if a sample containing a substoichiometric mixture of Cd^{II} with a mixture of $(CS\,L9C)_3$ and $(CS\,L19C)_3$ was examined, one observed the same two resonances ($\delta = 602$ and 628 ppm). These data suggest that thiolate exchange for Cd^{II}, like Hg^{II}, is slow on both the NMR and PAC timescales. However, Cd^{II}, which has a higher affinity for H_2O than Hg^{II}, exhibits a second, faster exchange process occurring in the range of μs to ns, a value consistent with the water exchange rates reported for solvated Cd^{II}.[46] The presence of only two species in the ^{199m}Hg PAC spectra that can be correlated to two ^{199}Hg NMR resonances corresponding to two different stoichiometries of sulfur bound to Hg^{II} suggests that water binding and exchange is not a significant process for Hg^{II} in these systems.

These studies have allowed us to gain a deeper understanding of the delicate interplay between Hg^{II} coordination and peptide fold preferences in determining the final overall structure of these metallopeptides. Together with our previous work,[30] they underscore the subtle balance that exits between obtaining the less favorable peptide aggregation state that contains the preferred Hg^{II} coordination geometry (Scheme 2, **A** and **B**) or the more favored peptide coiled-coil structure that contains the metal ion in an unusual coor-

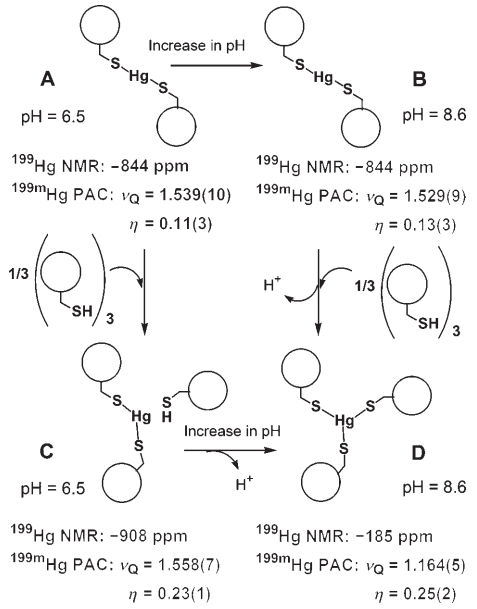

Scheme 2. Species present at different peptide/Hg^{II} ratios and pH values.

dination number (Scheme 2, **D**). As a consequence, the structure obtained under specific experimental conditions can be the result of a compromise situation between the high affinity of Hg^{II} to form dithiolate complexes and the affinity of the peptide to form a three-stranded coiled coil (Scheme 2, **C**). The existence of this interesting complex, [Hg{(TRI L9C)$_2$(TRI L9C−H)}], that contains a dithiolate–Hg^{II} ion encapsulated within a three-stranded coiled coil, highlights that at pH values lower than 8.5 coiled-coil formation is not the only factor that determines the stability of the trigonal thiolate–Hg^{II}. Therefore, the stabilization of this trigonal Hg^{II} complex at pH values lower than 8.5 cannot be achieved only by increasing the self-association energy of the coiled-coil formation, as it requires also the deprotonation of the third thiol inside the three-stranded coiled coil to generate the trigonal thiolate–Hg^{II}.

Given these observations, we can now consider mercury biochemistry more broadly by returning to the MerR system. Previous studies clearly showed that three of the four sulfurs in MerR were critical for complexation of Hg^{II}.[8,9] Furthermore, EXAFS and UV/Vis spectroscopy were consistent with a homoleptic $Hg^{II}S_3^-$ environment for the metal.[36,41] However, none of these approaches eliminates the possibility that a fourth cysteine thiol may bind as a weaker, thiol ligand in a HgS_3SH chromophore. The ^{199m}Hg PAC data presented here clearly rule out a significant binding interaction of this fourth potential thiol group. The excellent match to both the ν_Q and η values with our well-defined HgS_3 peptides demonstrates that neither the electric field gradient nor the symmetry of the MerR environment is consistent with any formulation other than the presently proposed symmetric trigonal Hg^{II} structure. One interesting issue to examine using both ^{199}Hg NMR and ^{199m}Hg PAC spectroscopic techniques would be the binding of Hg^{II} to MerR pre-bound to DNA as occurs naturally in the cells. All the current structural characterization has been performed on Hg^{II} bound to MerR without the DNA present. Only one ^{199}Hg NMR study was carried out that indicates practically no change in the ^{199}Hg NMR resonance of the system MerR–Hg upon binding of DNA.[10] However, adding Hg^{II} to MerR pre-bound to DNA, might produce different results.

Another biological system in which the combination of ^{199}Hg NMR and ^{199m}Hg PAC spectroscopy could provide beneficial results is in understanding copper homeostasis; for example, with the Atx1-like copper chaperones. Several groups have been studying copper homeostasis,[47–53] and it has been shown that Hg^{II} can be a good structural and functional model for Cu^I bound to these proteins.[19,54] Atx1-like copper chaperones and their target domains bind Cu^I with the two cysteine groups of the conserved MT/HCXXC motif. The Cd^{II}, Hg^{II}, and Cu^I crystal structures of Hah1, the Atx1 human homologue, reported by O'Halloran and Rosenzweig revealed, at pH 6.5, metal-ion coordination by two MT/HCXXC motifs.[55] These data indicated that Hg^{II} was bound as a trigonal HgS_3 structure and supported the proposal of a three-coordinate intermediate in the mechanism of Cu^I transfer in which this metal ion will be bound simultaneously by two MT/HCXX motifs, one corresponding to the metallochaperone and the other to its target protein. This proposal was further supported by the use of Cu^I in an NMR investigation by Banci et al.[52] The crystallographic data revealed important information regarding metal-ion specificity. The Cd^{II} ion coordinated to the four cysteines in a tetrahedral fashion, whereas Hg^{II} and Cu^I clearly bound to only three cysteines. Under their experimental conditions, Hg^{II} showed a weak secondary bonding interaction to the remaining fourth cysteine, whereas in the Cu^I crystal structure this type of interaction was not completely clear and the Cu^I site can be described as either three-coordinate with a weakly bound fourth cysteine or four-coordinate. Future pH-dependent ^{199m}Hg PAC and ^{199}Hg NMR spectroscopic studies could, in principle, determine whether the [Hg(Hah1)$_2$] dimer is capable of forming a four-coordinate center similar to that observed for Cd^{II} at higher pH (e.g., 7.6).

From the perspective of metalloprotein design, it is interesting to note that the ^{199}Hg NMR resonance ($\delta = -316$ ppm) observed for [Hg(TRI L19C)$_3$]$^-$, a **d**-substituted peptide, is markedly different from the resonance observed for the **a**-substituted peptide [Hg(TRI L9C)$_3$]$^-$ or MerR, yet the UV/Vis data for these three systems are very similar. This behavior was also observed for the closely related peptidic systems [Hg(CS L9C)$_3$]$^-$ and [Hg(CS L19C)$_3$]$^-$.[32] The $\delta = -316$ ppm feature could normally be associated with the presence of a fourth sulfur atom; however, the three peptide stoichiometry of the coiled coil eliminates this possibility. A more likely explanation is that this designed **d**-site is much more distorted than the **a**-site in TRI L9C. This hypothesis is consistent with the higher thiolate pK_a observed for Hg^{II}

binding to the **d**-peptides.[25,32] Future examination of this system using ^{199m}Hg PAC spectroscopy should easily resolve this issue.

Conclusion

In summary, we have probed for the first time the formation of the species [Hg{(TRI L9C)$_2$(TRI L9C-H)}], which contains a dithiolate–Hg^{II} complex in the interior of the hydrophobic core of the three-stranded coiled coil (TRI L9C)$_3$. The combination of the two powerful techniques, ^{199}Hg NMR and ^{199m}Hg PAC spectroscopy, has been crucial in demonstrating that the two dithiolate–Hg^{II} complexes, [Hg{(TRI L9C)$_2$(TRI L9C−H)}] and [Hg(TRI L9C)$_2$], are different. We have shown how in the first complex the presence of the third α-helix, containing the csyteine as a thiol group, breaks the symmetry of the environment present in the complex [Hg(TRI L9C)$_2$], resulting in distinct ^{199}Hg NMR and ^{199m}Hg PAC spectra. As pH is raised, the deprotonation of this third thiol generates the trigonal thiolate–Hg^{II} complex [Hg(TRI L9C)$_3$]$^-$. This equilibrium occurs on a timescale that is slower than the NMR timescale (0.01–10 ms), and contrasts with the faster water exchange ($\approx 10^6$–10^8 s^{-1}) observed for different Cd^{II} complexes of the TRI peptides. Thus, we have shown that the combination of ^{199}Hg NMR and ^{199m}Hg PAC spectroscopy can be broadly used to distinguish not only static structures, but also between exchange processes on very different timescales. These studies represent a successful application of the combination of ^{199}Hg NMR and ^{199m}Hg PAC spectral data in determining the structure of Hg^{II} bound to three- and two-stranded coiled coils. They can be extended to further clarifying metal binding to and transfer between the native proteins of the MerR system and to study the mechanisms of copper homeostasis. Considering the different timescale of both spectroscopic methods and their sensitivity to different Hg^{II} environments, their parallel use can result in a potent tool to study Hg interactions with different biomolecules and gain crucial information regarding the structural, kinetic, and thermodynamic details of these interactions. These type of studies can help in unraveling the molecular basis for Hg^{II} toxicity and their environmental effects.

Experimental Section

Peptide synthesis and purification: The peptides TRI L9C (Ac-G LKALEEK**C**KALEEK LKALEEK LKALEEK G-NH$_2$) and TRI L19C (Ac-G LKALEEK LKALEEK LKA**C**EEK LKALEEK G-NH$_2$) were synthesized on an Applied Biosystems 433 A peptide synthesizer using standard protocols,[56] and purified and characterized as described previously.[30]

UV/Vis spectroscopy: All the spectra were collected at room temperature on a Carey 100 Bio UV/Vis Spectrophotometer. Fresh solutions of the purified peptide were prepared for each experiment using doubly distilled water and were purged with argon to minimize the chances of oxidation. The peptide concentration was determined by quantification of the cysteine thiols by using the Ellman's test.[57] Equivalent amounts of peptide were added to two solutions: the sample, containing $HgCl_2$ (3 mL, 20 μM $HgCl_2$) in phosphate buffer (50 mM) at pH 6.5; and the reference solution, containing only the buffer. After peptide addition, the solutions were left to equilibrate for 15 min before a difference spectrum was collected.

^{199}Hg NMR spectroscopy: All the spectra were collected at room temperature on a Varian Inova 500 spectrometer (89.48 MHz for ^{199}Hg) equipped with a 5 mm broadband probe. ^{199}Hg NMR spectra were externally referenced to a 0.1 M $Hg(ClO_4)_2$ in a 0.1 M $HClO_4/D_2O$ solution at −2250 ppm.[58] A spectral width of 1340 ppm (119.940 Hz) was sampled using a 6.0 μs 90° pulse and 0.01 s acquisition time with a delay between scans of 0.005 s. Samples were prepared under a flow of argon by dissolving the lyophilized and degassed peptides TRI L9C and TRI L19C (20–30 mg) in 340 μL and 100 μL 15% D_2O solution, respectively. The peptide concentrations were determined by using the Ellman's test.[57] The final samples were prepared by the addition of the appropriate amount of $^{199}Hg(NO_3)_2$ (125 mM stock solution prepared from 91% isotopically enriched ^{199}HgO obtained from Oak Ridge National Laboratory) and the adjustment of the pH with KOH or HCl solutions. An argon atmosphere was maintained when possible, but the samples came in contact with O_2 while the pH was adjusted. The actual final concentrations for each experiment are indicated in the result section and figure captions. The data were analyzed by using the software MestRe-C.[59] All free induction decays (FID's) were zero filled to double the original points and were processed by application of 100 Hz line broadening prior to Fourier transformation.

Perturbed angular correlation spectroscopy: The following stock solutions were prepared and used for the PAC experiments: TRI L9C (2.5 mM, concentration determined by the Ellman's test[57]), phosphate buffer pH 8.0 (0.82 M for samples at pH 7.9, 8.1 and 8.7), phosphate buffer pH 6.3 (0.93 M for samples at pH 6.5 and 6.6), and $HgCl_2$ (3.0 mM). The final samples contained 30–40 mM of the proper buffer, 125–130 μM TRI L9C and the appropriate amount of $HgCl_2$ solution to achieve the ratios shown in Table 1. Water (150 μL) treated so as to lower the concentration of metal ions was placed in a small teflon cup sitting on a copper device, frozen in liquid nitrogen and mounted at the ISOLDE GLM beam line (at CERN) in a vacuum chamber. Radioactive ^{199m}Hg was implanted in the ice typically for 1 hour. The radioactive ^{199m}Hg ($t_{1/2}$ = 43 min, half-life of intermediate nuclear state = 2.3 ns) was produced by irradiating a liquid lead target with 1 GeV protons and selected using an on line mass separator. The ice was thawed slowly ($\approx$10 min) in a fume hood so as to minimize the risk of contamination from mercury vapour, and under an argon atmosphere in order to avoid condensation of water vapour from the air. Mercury(II) chloride, buffer solution and peptide were added in that order to the ^{199m}Hg containing sample. The pH value of the final solution was adjusted using KOH (0.25 M) or HCl (0.25 M) stock solutions. A parallel sample, identical to the actual sample but without the radioactive ^{199m}Hg, was prepared and used to determine the needed volume of KOH or HCl to achieve the desired pH. This procedure was adopted in order to save time when working with the actual sample. The pH reported in Table 1 was measured in the actual sample at room temperature after the PAC experiment and corrected to pH at 1 °C by using http://www.liv.ac.uk/buffers/buffercalc.html. After pH adjustment, the sample was left to incubate for 10 min and finally sucrose was added to 55% w/w in order to reduce the Brownian tumbling of the molecules. The sample temperature was controlled by a Peltier element, and all PAC experiments were carried out at 1 °C. PAC data collection was initiated after 5 min allowing for thermal equilibration at 1 °C.

The PAC instrument is a 6-detector PAC camera as described by Butz et al.,[60] and data collection and analysis was carried out by using the software Prelude and Winfit (developed by T. Butz and co-workers, University of Leipzig) with a standard chi-square algorithm. The instrument time resolution and time calibration were determined to be 0.846 ns (full width at half maximum) and 0.04955 ns per channel, respectively. Copper cups were placed at the front end of the detectors absorbing a large fraction of the 80 keV X-rays also emitted from the radioactive mercury. All fits were carried out with 400 data points, disregarding the 3–5 first points due to systematic errors in these. Using ^{199m}Hg in solution the

spectra were adjusted such that a specific time delay between the two γ-rays occurred in the same channel in all spectra (t_0 determination). A Lorentzian line shape was assumed, but otherwise the data-analysis was identical to that described in Hemmingsen et al.[61] Each nuclear quadrupole interaction (NQI) was modeled by using a separate set of parameters that included ν_Q, η, δ, $1/\tau_c$, and A. The parameter ν_Q [$\nu_Q = eQV_{zz}/h$, in which Q is the nuclear electric quadrupole moment and V_{zz} is the numerically largest eigenvalue of the electric field gradient tensor] is associated with the strength of the interaction between the surrounding electronic environment and the Hg nucleus; η is the so-called asymmetry parameter which is 0 in an axially symmetric complex and has a maximal value of 1; δ is the relative frequency spread; τ_c is the rotational correlation time; and A is the amplitude of the signal (see reference [22] for a more detailed description). As ν_Q does not directly give the frequencies exhibited in the PAC spectra, we also report the parameter ω_1, the frequency at which the first peak in the Fourier transform is located (see reference [62] for a more detailed description). In all cases in which two NQIs were fitted the rotational correlation time was constrained to be the same for the two signals. The parameters fitted to the PAC data are presented in Table 1.

Acknowledgements

We thank ISOLDE collaboration at CERN for the ^{199m}Hg beam time grant (experiment IS448). V.L.P. thanks the National Institute of Health for support of this research (R01 ES0 12236) and O.I. thanks the Margaret and Herman Sokol Foundation for a Postdoctoral Award.

[1] B. L. Vallee, D. D. Ulmer, *Annu. Rev. Biochem.* **1972**, *41*, 91–128.
[2] I. Onyido, A. R. Noriis, E. Buncel, *Chem. Rev.* **2004**, *104*, 5911–5929.
[3] M. J. Natan, C. F. Millikan, J. G. Wright, T. V. O'Halloran, *J. Am. Chem. Soc.* **1990**, *112*, 3255–3257.
[4] M. Satoh, N. Nishimura, Y. Kanayama, A. Naganuma, T. Suzuki, C. Tohyama, *J. Pharmacol. Exp. Ther.* **1997**, *283*, 1529–1533.
[5] J. G. Wright, M. J. Natan, F. M. MacDonnell, D. M. Ralston, T. V. O'Halloran, *Prog. Inorg. Chem.* **1990**, *38*, 323–412.
[6] T. Barkay, S. M. Miller, A. O. Summers, *FEMS Microbiol. Rev.* **2003**, *27*, 355–384.
[7] J. L. Hobman, J. Wilkie, N. L. Brown, *BioMetals* **2005**, *18*, 429–436.
[8] L. M. Shewchuck, G. L. Verdine, C. T. Walsh, *Biochemistry* **1989**, *28*, 2331–2339.
[9] J. D. Helmann, B. T. Ballard, C. T. Walsh, *Science* **1990**, *247*, 946–948.
[10] L. M. Utschig, J. W. Bryson, T. V. O'Halloran, *Science* **1995**, *268*, 380–385.
[11] D. M. Ralston, T. O'Halloran, *Proc. Natl. Acad. Sci. USA* **1990**, *87*, 3846–3850.
[12] P. B. Blake, M. F. Summers, *Adv. Inorg. Biochem.* **1994**, *10*, 201–228.
[13] D. L. Huffman, L. M. Utschig, T. O'Halloran, in *Metal Ions in Biological Systems, Vol. 34* (Eds.: A. Sigel, H. Sigel), Dekker, New York, **1997**, pp. 503–527.
[14] D. C. Bebout, S. M. Berry, *Struct. Bonding (Berlin)* **2006**, *120*, 81–105.
[15] R. A. Steele, S. J. Opella, *Biochemistry* **1997**, *36*, 6885–6895.
[16] G. Veglia, F. Porcelli, T. DeSilva, A. Prantner, S. J. Opella, *J. Am. Chem. Soc.* **2000**, *122*, 2389–2390.
[17] L. M. Utschig, J. G. Wright, G. R. Dieckmann, V. L. Pecoraro, T. V. O'Halloran, *Inorg. Chem.* **1995**, *34*, 2497–2498.
[18] L. M. Utschig, T. Baynard, C. Strong, T. V. O'Halloran, *Inorg. Chem.* **1997**, *36*, 2926–2927.
[19] R. A. Pufahl, C. P. Singer, K. L. Peariso, S.-J. Lin, P. J. Schmidt, C. J. Fahrni, V. C. Culotta, J. E. Penner-Hahn, T. V. O'Halloran, *Science* **1997**, *278*, 853–856.
[20] P. B. Blake, B. Lee, M. F. Summers, J.-B. Park, Z. H. Zhou, M. W. W. Adams, *New J. Chem.* **1994**, *18*, 387–395.
[21] J. L. Sudmeier, T. G. Perkins, *J. Am. Chem. Soc.* **1977**, *99*, 7732–7733.
[22] L. Hemmingsen, K. Narcisz, E. Danielsen, *Chem. Rev.* **2004**, *104*, 4027–4061.
[23] W. Tröger, T. Butz, *Hyperfine Interact.* **2000**, *129*, 511–527.
[24] C. Lippert, W. Tröger, T. Butz, in *30th Zakopane School of Physics* (Eds.: K. Tomala, E. A. Gorlich), Krakow, Poland, **1995**.
[25] M. Matzapetakis, B. T. Farrer, T.-C. Weng, L. Hemmingsen, J. E. Penner-Hahn, V. L. Pecoraro, *J. Am. Chem. Soc.* **2002**, *124*, 8042–8054.
[26] K. H. Lee, M. Matzapetakis, S. Mitra, E. N. G. Marsh, V. L. Pecoraro, *J. Am. Chem. Soc.* **2004**, *126*, 9178–9179.
[27] K.-H. Lee, C. Cabello, L. Hemmingsen, E. N. G. Marsh, V. L. Pecoraro, *Angew. Chem.* **2006**, *118*, 2930–2934; *Angew. Chem. Int. Ed.* **2006**, *45*, 2864–2868; .
[28] G. R. Dieckmann, D. K. McRorie, D. L. Tierney, L. M. Utschig, C. P. Singer, T. V. O'Halloran, J. E. Penner-Hahn, W. F. DeGrado, V. L. Pecoraro, *J. Am. Chem. Soc.* **1997**, *119*, 6195–6196.
[29] G. R. Dieckmann, D. K. McRorie, J. D. Lear, K. A. Sharp, W. F. DeGrado, V. L. Pecoraro, *J. Mol. Biol.* **1998**, *280*, 897–912.
[30] B. T. Farrer, N. P. Harris, K. E. Balchus, V. L. Pecoraro, *Biochemistry* **2001**, *40*, 14696–14705.
[31] D. Ghosh, K.-H. Lee, B. Demeler, V. L. Pecoraro, *Biochemistry* **2005**, *44*, 10732–10740.
[32] O. Iranzo, D. Ghosh, V. L. Pecoraro, *Inorg. Chem.* **2006**, *45*, 9959–9973.
[33] G. Christou, K. Folting, J. C. Huffman, *Polyhedron* **1984**, *3*, 1247–1253.
[34] E. S. Gruff, S. A. Koch, *J. Am. Chem. Soc.* **1990**, *112*, 1245–1247.
[35] T. Alsina, W. Clegg, K. A. Fraser, J. Sola, *J. Chem. Soc. Dalton Trans.* **1992**, 1393–1399.
[36] S. P. Watton, J. G. Wright, F. M. MacDonnell, J. W. Bryson, M. Sabat, T. O'Halloran, *J. Am. Chem. Soc.* **1990**, *112*, 2824–2826.
[37] T. Butz, W. Tröger, T. Pohlmann, O. Nuyken, *Z. Naturforsch. A* **1992**, *47*, 85–88.
[38] G. R. Dieckmann, PhD thesis, University of Michigan (Ann Arbor), **1995**.
[39] W. Tröger, *Hyperfine Interact.* **1999**, *120/121*, 117–128.
[40] W. Tröger, T. Butz, P. Blaha, K. Schwarz, *Hyperfine Interact.* **1993**, *80*, 1109–1116.
[41] J. G. Wright, H.-T. Tsang, J. E. Penner-Hahn, T. V. O'Halloran, *J. Am. Chem. Soc.* **1990**, *112*, 2434–2435.
[42] L. Hemmingsen, U. Ryde, R. Bauer, *Z. Naturforsch. A* **1999**, *54*, 422–430.
[43] N. j. Taylor, A. J. Carty, *J. Am. Chem. Soc.* **1977**, *99*, 6143–6145.
[44] B. V. Cheesman, A. P. Arnold, D. L. Rabenstein, *J. Am. Chem. Soc.* **1988**, *110*, 6359–6364.
[45] M. Matzapetakis, V. L. Pecoraro, *J. Am. Chem. Soc.* **2005**, *127*, 18229–18233.
[46] Y. Docommun, A. E. Merbach, in *Inorganic High Pressure Chemistry: Kinetics and Mechanisms* (Ed.: R. V. Eldik), Elsevier, Amsterdam, **1986**, p. 70.
[47] D. L. Huffman, T. O'Halloran, *Annu. Rev. Biochem.* **2001**, *70*, 677–701.
[48] A. C. Rosenzweig, *Acc. Chem. Res.* **2001**, *34*, 119–128.
[49] F. Arnesano, L. Banci, I. Bertini, F. Cantini, S. Ciofi-Baffoni, D. L. Huffman, T. V. O'Halloran, *J. Biol. Chem.* **2001**, *276*, 41365–41376.
[50] L. Banci, A. Rosato, *Acc. Chem. Res.* **2003**, *36*, 215–221.
[51] F. Arnesano, L. Banci, I. Bertini, A. M. J. J. Bonvin, *Structure* **2004**, *12*, 669–676.
[52] L. Banci, I. Bertini, F. Cantini, I. C. Felli, L. Gonnelli, N. Hadjiliadis, R. Pierattelli, A. Rosato, P. Voulgaris, *Nat. Chem. Biol.* **2006**, *2*, 367–368.
[53] E. Gaggelli, H. Kozlowski, D. Valensin, G. Valensin, *Chem. Rev.* **2006**, *106*, 1995–2044.
[54] A. C. Rosenzweig, D. L. Huffman, M. Y. Hou, A. K. Wernimont, R. S. Pufahl, T. V. O'Halloran, *Structure* **1999**, *7*, 605–617.
[55] A. K. Wernimont, D. L. Huffman, A. L. Lamb, T. V. O'Halloran, A. C. Rosenzweig, *Nat. Struct. Biol.* **2000**, *7*, 766–771.

[56] W. C. Chan, P. D. White, *Fmoc Solid Phase Peptide Synthesis: A Practical Approach*, Oxford University Press, New York, **2000**.
[57] G. M. Ellman, *Arch. Biochem. Biophys.* **1959**, *82*, 70–77.
[58] B. Wrackmeyer, R. Contreras, *Annu. Rep. NMR Spectrosc.* **1992**, *24*, 267–329.
[59] C. Cobas, J. Cruces, F. J. Sardina, MestRe-C version 2.3, Universidad de Santiago de Compostela, Spain, **2000**.
[60] T. Butz, S. Saibene, T. Fraenzke, M. Weber, *Nucl. Instrum. Methods Phys. Res. Sect. A* **1989**, *284*, 417–421.
[61] L. Hemmingsen, R. Bauer, M. J. Bjerrum, M. Zeppezauer, H. W. Adolph, G. Formicka, E. Cedergren-Zeppezauer, *Biochemistry* **1995**, *34*, 7145–7153.
[62] T. Butz, *Hyperfine Interact.* **1989**, *52*, 189–228.
[63] P. Faller, B. Ctortecka, W. Tröger, T. Butz, M. Vasek, *J. Biol. Inorg. Chem.* **2000**, *5*, 393–401.

Received: August 2, 2007
Published online: October 25, 2007

